Dalton Transactions

Catalytic Dinitrogen Reduction to Hydrazine and Ammonia using $Cr(N_2)_2(diphosphine)_2$ Complexes

Journal:	*Dalton Transactions*
Manuscript ID	DT-COM-03-2024-000702
Article Type:	Communication
Date Submitted by the Author:	08-Mar-2024
Complete List of Authors:	Beasley, Charles; Montana State University Bozeman, Chemistry and Biochemistry Duletski, Olivia; Montana State University Bozeman, Chemistry and Biochemistry Stankevich, Ksenia; Montana State University Bozeman, Chemistry and Biochemistry Arulsamy, Navamoney; University of Wyoming, Chemistry Mock, Michael; Montana State University Bozeman, Chemistry and Biochemistry

COMMUNICATION

Catalytic Dinitrogen Reduction to Hydrazine and Ammonia using $Cr(N_2)_2(diphosphine)_2$ Complexes

Received 00th January 20xx,
Accepted 00th January 20xx

DOI: 10.1039/x0xx00000x

www.rsc.org/

Charles H. Beasley,[a] Olivia L. Duletski,[a] Ksenia S. Stankevich,[a] Navamoney Arulsamy,[b] and Michael T. Mock[a,*]

The synthesis, characterization of *trans*-$[Cr(N_2)_2(depe)_2]$ (1) is described. 1 and *trans*-$[Cr(N_2)_2(dmpe)_2]$ (2) catalyze the reduction of N_2 to N_2H_4 and NH_3 in THF using SmI_2 and H_2O or ethylene glycol as H^+ sources. 2 produces the highest total fixed N for a molecular Cr catalyst to date.

Motivated by the desire to understand and control the challenging multi-proton, multi-electron reaction of N_2 reduction to NH_3, researchers have intensely studied the reactivity of molecular transition metal dinitrogen complexes.[1] Well-defined molecular systems offer a high degree of electronic and structural control to regulate chemical reactivity of N_2.[2] When combined with effective strategies to form N–H bonds, such as proton-coupled electron transfer (PCET) reagents[3], i.e. SmI_2 and a proton source, tens-of-thousands of equivalents of NH_3 can be generated.[4] The valuable information obtained from these studies includes the identification of viable $M–N_xH_y$ reaction intermediates from spectroscopic data that can be used to delineate the mechanistic steps of a putative catalytic cycle. Such studies can aid in the understanding of the mechanistically complex biological N_2 fixation processes carried out by nitrogenase enzymes[5], as well as heterogeneous Haber-Bosch catalysts.[6]

Group 6 N_2 complexes bearing monodentate phosphine ligands, especially with Mo and W, were among the first molecular systems to generate stoichiometric quantities of N_2-derived NH_3 from protonolysis reactions with strong acids nearly 50 years ago.[7] Recently, a renaissance of examining structurally similar $[M(N_2)_2(P–P)_2]$, (M = Mo, W; P–P = diphosphine) systems has begun, elevating these simple complexes as catalysts for N_2 reduction to NH_3, or other remarkable reactions such as cleavage of the N_2 triple bond.[8] Masuda and co-workers reported spontaneous N≡N bond cleavage upon one-electron oxidation of *trans*-$[Mo(N_2)_2(depe)_2]$ (depe = $Et_2PCH_2CH_2PEt_2$) to form $[Mo(N)(depe)_2]^+$.[9] Chirik and co-workers developed a photocatalytic strategy to form NH_3 from $[Mo(N)(depe)_2]^+$ and H_2.[10] Electrocatalytic N_2 fixation with Mo and W-phosphine complexes was described by Peters and co-workers using a tandem catalysis approach.[11] Nishibayashi and co-workers showed simple Mo-phosphine complexes catalyzed N_2 reduction to NH_3 using SmI_2 and various H^+ sources.[12]

While these examples highlight new discoveries using $[M(N_2)_2(P–P)_2]$ (M = Mo, W) complexes, catalytic N_2 reduction with analogous Cr compounds are limited. Recent reports highlighted the utility of molecular Cr complexes using a variety of ligand architectures for N_2 activation,[8a, 13] functionalization,[14] or catalytic N_2 silylation.[15] However, molecular Cr complexes that catalyze the direct reduction of N_2 to NH_3 are rare. In 2022, Nishibayashi and co-workers reported a Cr complex bearing a PCP pincer ligand that catalyzed direct N_2 reduction to NH_3 and N_2H_4 at −78 °C to rt. KC_8 and phosphonium salts as H^+ sources were required for turnover, and this system was not catalytic using SmI_2.[16] Herein we prepared and characterized *trans*-$[Cr(N_2)_2(depe)_2]$ (**1**), and report catalytic N_2 reduction to NH_3 using **1** and *trans*-$[Cr(N_2)_2(dmpe)_2]$[17] (**2**) (dmpe = $Me_2PCH_2CH_2PMe_2$) at 25 °C using SmI_2 with ethylene glycol or H_2O as proton sources.

Vigorous stirring of yellow *trans*-$[CrCl_2(depe)_2]$[18] (**1-Cl**) in THF with excess Mg powder under a N_2 atmosphere for 24 h furnished *trans*-$[Cr(N_2)_2(depe)_2]$ as a dark red solid in 70% yield. Isolation of **1** allowed for a comparison of the structural and spectroscopic data with **2** that was reported in 1983.[17a] The structure of **1**, determined by single crystal X-ray diffraction, shows Cr with four phosphorus atoms of the chelates on the equatorial plane and two axial end-on bound N_2 ligands, Fig. 1, panel a. The average Cr–N, Cr–P, and N≡N bond distances are 1.904 ±0.005 Å, 2.334 ±0.007 Å, and 1.104 ±0.004 Å, respectively. The corresponding Cr–N, and Cr–P, bond distances in **2** (See ESI†), are slightly shorter at 1.8862(17) Å, and 2.294 ±0.005 Å, and the N≡N distance is 1.110(2) Å.[19]

[a] *Department of Chemistry and Biochemistry, Montana State University, Bozeman, MT 59717, USA. E-mail: michael.mock@montana.edu*
[b] *Department of Chemistry, University of Wyoming, Laramie, WY, 82071, USA.*

† Electronic Supplementary Information (ESI) available: Experimental procedures, crystallographic details, and additional spectroscopic and electrochemical data. CCDC 2330754 (**1**), 2330755 (**2**). For ESI and crystallographic data in CIF or other electronic format see DOI: 10.1039/x0xx00000x

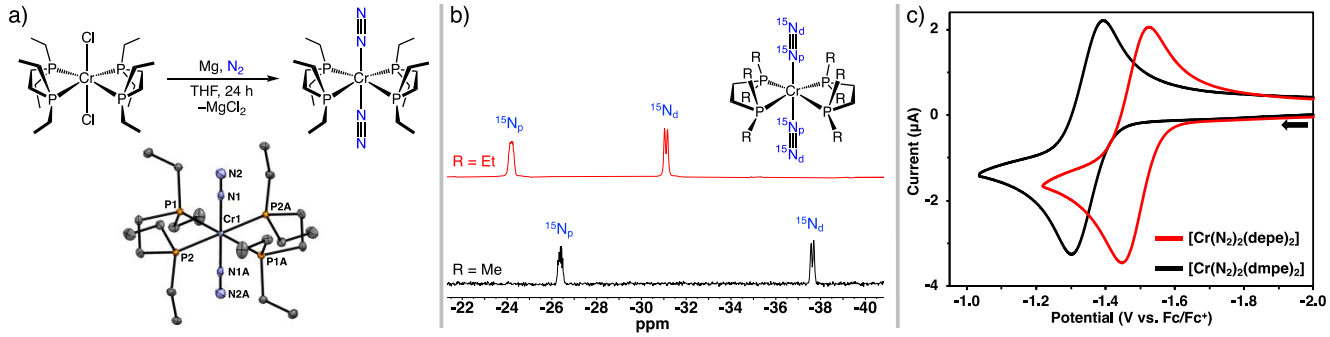

Fig. 1 (a) Synthesis and molecular structure of **1.** Thermal ellipsoids are drawn at 50% probability. Hydrogen atoms are omitted for clarity. Crystals of **1** contain two molecules per asymmetric unit with comparable metric parameters; only one molecule is shown. Selected bond distances (Å) and angles (°): Cr1–N1 = 1.9081(10); N1–N2 = 1.1003(14); Cr–P1 = 2.3343(3); Cr–P2 = 2.3249(3). Cr2–N3 = 1.9008(10); N3–N4 = 1.1069(14); Cr–P3 = 2.3425(3); Cr–P4 = 2.3346(3). P1–Cr1–P2 = 81.650(9); P3–Cr2–P4 = 81.583(10); P1–Cr1–N1 = 89.25(3); P2–Cr1–N1 = 90.21(3); P3–Cr2–N3 = 89.29(3); P4–Cr2–N3 = 90.59(3). (b) $^{15}N\{^1H\}$ NMR spectra of $\mathbf{1}^{15N}$ (red) and $\mathbf{2}^{15N}$ (black) recorded at 25 °C in THF-d_8. (c) Cyclic voltammograms of **1** and **2** in THF showing the $Cr^{I/0}$ wave.

In each case, the ligand bite angles for **1** and **2**, i.e. P1–Cr–P2, are 81.6° and 83.5°, respectively, and the P–Cr–N angles are near 90°. The $^{31}P\{^1H\}$ NMR spectrum of **1** in THF-d_8, displays a singlet at 79.9 ppm (68.8 ppm for **2**) consistent with four magnetically equivalent P atoms. Complexes **1** and **2** were characterized by ^{15}N NMR spectroscopy to augment the cumulative library of tabulated ^{15}N NMR data of phosphine-supported group 6 N_2 complexes.[13h] The $^{15}N_2$-labelled complexes $\mathbf{1}^{15N}$ and $\mathbf{2}^{15N}$, were prepared by mixing the respective Cr-N_2 complexes in THF-d_8 under 1 atm $^{15}N_2$. The ^{15}N NMR data was collected after mixing for 24 h. The $^{15}N\{^1H\}$ NMR spectra contain two resonances; a doublet (J_{NN} = 7.0 Hz) and a multiplet (~2.5 Hz ^{31}P coupling) ($\mathbf{1}^{15N}$: –24.2 ppm, –31.1 ppm, and $\mathbf{2}^{15N}$: –26.4 ppm, –37.6 ppm), assigned as the proximal (N_p) and distal (N_d) nitrogen atoms, respectively, (Fig. 1, panel b).[13i]

Cyclic voltammetry (CV) experiments established the redox behaviour of the Cr(0)-N_2 complexes. Voltammograms were recorded using a glassy carbon working electrode at 0.1 V s^{-1} in THF. Each complex displays a reversible, one-electron $Cr^{I/0}$ wave with the half-wave potential ($E_{1/2}$) of –1.49 V and –1.34 V (vs. $Cp_2Fe^{+/0}$) for **1** and **2**, respectively (Fig. 1, panel c). The electrochemically reversible $Cr^{I/0}$ couples indicate N_2 dissociation does not occur upon oxidation to Cr(I) during the CV experiments. The reversibility of the waves for **1** and **2** contrasts other *cis*- or *trans*-$[Cr(N_2)_2(P_4)]$ complexes measured by CV that exhibit quasi-reversible or irreversible $Cr^{I/0}$ waves due to rapid N_2 loss upon oxidation.[13b, 13c, 13i] In the current study, an irreversible anodic wave was assigned to the $Cr^{II/I}$ redox feature at E_{pa} = −0.48 V and E_{pa} = −0.63 V, for **1** and **2**, respectively, due to N_2 dissociation at more positive potentials, (Fig. S16, S17 ESI†). The CV data suggests one-electron chemical oxidation to form *trans*-$[Cr(N_2)_2(P\text{-}P)_2]^+$ should be possible; however, our attempts to *isolate* such a species have been unsuccessful. Owing to the more electron-rich metal centre of **1**, the ν_{NN} band in the infrared spectrum at 1906 cm^{-1} (THF) appears at lower energy than the ν_{NN} band for **2** at 1917 cm^{-1} (THF).

Complexes **1** and **2** were examined as catalysts for the direct reduction of N_2 to NH_3 and N_2H_4. The catalysis studies were performed in THF at room temperature using the PCET reagent SmI_2 and ethylene glycol and/or water as proton donors. A typical catalytic run used 583 equiv SmI_2, 1166 equiv ROH per Cr centre and was stirred for 48 h. Quantification of NH_3, N_2H_4 and H_2 (see ESI for details†) products assessed the total fixed N generated in each reaction. Selected catalytic data are listed in Table 1 (see ESI for all tabulated results†).

Table 1. Selected Cr-catalyzed N_2 reduction experiments.

$$N_2 + SmI_2 + ROH \xrightarrow[THF,\ rt]{[Cr]\ cat.} NH_3 + N_2H_4 + H_2$$

Entry	Cr cat.	ROH	NH_3 equiv/Cr[a]	N_2H_4 equiv/Cr[b]	Total Fixed N	Time (h)
1	none	$(CH_2OH)_2$	0	0	0	48
2	**1**	$(CH_2OH)_2$	3.7 ± 0.9	1.4 ± 0.8	4.9[h]± 1.5	48
3	**1**	$(CH_2OH)_2$	4.6 ± 0.6	4.0 ± 1.7	8.6[h] ± 2.1	100
4[c]	**1**	H_2O	1.4	0.7	2.1	48
5[d]	**1**	H_2O	3.2	0.6	3.8	28
6	**1-Cl**	$(CH_2OH)_2$	1.2	0.9	2.1	48
7	**2**	$(CH_2OH)_2$	14.6 ± 1.6	5.9 ± 2.9	20.5[h]± 3.8	48
8[e]	**2**	$(CH_2OH)_2$	6.2 ± 0.5	6.4 ± 0.8	12.6[h] ± 0.3	48
9[f]	**2**	$(CH_2OH)_2$	4.4 ± 0.9	6.6 ± 0.6	11[h]± 0.4	48
10[g]	**2**	$(CH_2OH)_2$	1.1	5.7	6.8	48
11[d]	**2**	H_2O	5.1	5.9	11	3
12	**2-Cl**	$(CH_2OH)_2$	13.5 ± 2.8	5.9 ± 0.6	19.4[h]± 3.4	48

Experiments performed using 0.6 μmol catalyst in 15.0 mL THF at 25 °C under 1 atm N_2, with 583 equiv of SmI_2, and with 1166 equiv ROH unless otherwise specified. [a]determined by acidification and NH_4^+ quantification using ^1H NMR spectroscopy (see ESI). [b]determined by colormetric p-dimethylaminobenzaldehyde method (see ESI). [c]1000 equiv H_2O/Cr; [d]10,000 equiv H_2O/Cr; [e]25 ppm of H_2O. [f]250 ppm of H_2O. [g]583 equiv $(CH_2OH)_2$, 583 equiv H_2O. [h]Average of two or more trials. H_2 quantification by gas chromatography, values are tabulated in ESI.

Analysis of the catalytic data provides insights about the performance of **1** and **2** under identical reaction conditions. **2** afforded more total fixed N than **1** in all catalytic trials. For example, **1** generated up to 5 equiv of NH_3 *and* 5 equiv N_2H_4 per Cr center using ethylene glycol as the proton

donor after >100 h. Under identical conditions, **2** produced up to 16 equiv NH_3 *and* 10 equiv N_2H_4 in 48 h. Furthermore, ethylene glycol worked more effectively as the proton donor affording higher total fixed N than using H_2O. The deliterious effect of H_2O on catalysis was noted in reactions with **2** using ethylene glycol as the primary proton source. As the amount of H_2O added to the reaction increased, NH_3 production declined, while the N_2H_4 formed stayed relatively constant. We postulate the Cr complexes may simply be more prone to degradation in the presence of H_2O. Separately, **2** was treated with 500 equiv H_2O or ethylene glycol in THF-d_8. Free dmpe from complex degradation appeared more rapidly using H_2O, as assessed by ^{31}P NMR spectroscopy. Catalysis performed with **2-^{14}N** under an atmosphere of $^{15}N_2$ afforded $^{15}NH_4^+$ as a doublet at 7.1 ppm ($J_{15N\text{-}1H}$ = 71 Hz) in the ^{1}H NMR spectrum, identifying $^{15}N_2$ as the source of $^{15}NH_3$.

Catalytic trials using *trans*-[$CrCl_2$(dmpe)$_2$] (**2-Cl**) and ethylene glycol generated comparable amounts of NH_3 *and* N_2H_4 as using **2** as the precatalyst. **1-Cl** did not catalyze N_2 reduction, affording only 1 equiv of NH_3 *and* N_2H_4 per Cr center. SmI_2 and ethylene glycol may be ineffective at reducing the Cr(II) center of **1-Cl** to Cr(0) where N_2 is strongly activated. Treatment of **2-Cl** with 2 equiv SmI_2 and 2 equiv ethylene glycol rapidly generated **2** (See ESI). However, the same reaction of **1-Cl** and SmI_2 with ethylene glycol additive did not form **1** ($E_{1/2}$ = −1.49 V, *vide supra*). **1** or **2** could not be generated from **1-Cl** or **2-Cl** using excess SmI_2(THF) alone ($E°$ of SmI_2(THF) = −1.41 ± 0.08 V[20] vs. Fc/Fc^+). A Cr(I) species could be accessible, but N_2 activation and subsequent functionalization steps may be moderated at Cr(I), limiting catalysis.

The mixed N_2 reduction selectivity to form NH_3 *and* N_2H_4 provides preliminary evidence for a catalytic cycle that follows, at least in part, an alternating N_2 reduction mechanism, Fig. 2, bottom. A purely distal N_2 reduction pathway, Fig. 2, top, would be selective for NH_3 formation. In a 1986 report, the reaction of **2** with CF_3SO_3H was potulated to form a Cr-hydrazido product, $[Cr{=}N{-}NH_2]^+$.[21]

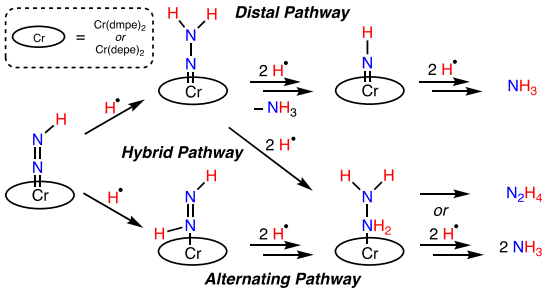

Fig. 2 Plausible N_2 reduction mechanisms for Cr mediated formation of hydrazine and ammonia.

A recent study by Wei, Yi, Xi, and co-workers examining early stage N_2 functionalization of $[Cp^*Cr^0(depe)(N_2)]^-$ (Cp^* = $C_5(CH_3)_5$) using a variety of electrophiles (H^+, Me_3Si^+, Me^+) also revealed the selective formation of Cr-hydrazido products, consistent with a distal pathway. Contrary to these reaction patterns, protonation studies of related *cis*- or *trans*-[$Cr(N_2)_2(P_4)$] complexes we examined using strong acids or H^+/e^- reagents, as well as the catalytic Cr[PCP] system[16] generated NH_3 *and* N_2H_4.[13c, 13i, 15a] Considering all these examples, and that N_2 reduction mechanisms are sensitive to reaction conditions, (i.e. identity of the H^+ and e^- reagents, solvent, temperature), a hybrid N_2 reduction pathway[22] where the third and fourth N−H bonds form at the proximal N atom of a Cr-hydrazido intermediate, Fig. 2, middle, cannot be excluded for the current systems. Further studies are warranted to understand the N_2 reduction pathways with Cr.

The proclivity for N_2 ligand substitution in **1** and **2** was evaluated as a metric that could reflect catalyst stability and influence catalytic performance. We examined reactions of **1** and **2** with CO to assess the rate of ligand exchange, Fig. 3. Ligand substitution in these six-coordinate complexes is expected to be a dissociative process; a result of Cr−N or Cr−P bond dissociation. Wilkinson, Hursthouse, and co-workers noted **2** did not react with 7 atm CO for several hours except under u.v. irradiation (in light petroleum) to form *cis*-[$Cr(CO)_2$(dmpe)$_2$] (***cis*-2-CO**).[17b] This account was surprising, and the unreactive nature toward N_2/CO exchange seemed uncharacteristic of a complex with terminally bound N_2 ligands. We reacted **2** with 1 atm CO at 25 °C in pentane or THF without u.v. irradiation and monitored the reaction by in situ IR spectroscopy, or ^{31}P NMR spectroscopy (see ESI†). In both solvents the reaction was slow, but **2** was not unreactive. In THF, after 26 h ~85% of **2** converted to a ~1:1 mixture of ***cis*-2-CO** and *trans*-[$Cr(CO)_2$(dmpe)$_2$] (***trans*-2-CO**). ***trans*-2-CO** converts to ~95% ***cis*-2-CO** (and ~3% free dmpe) after additional 46 h by ^{31}P NMR spectroscopy. In THF, **1** converts directly to *cis*-[$Cr(CO)_2$(depe)$_2$] ***cis*-1-CO** (ν_{CO} = 1829, 1768 cm^{-1}) in ~3 h by in situ IR spectroscopy (see ESI†). The vastly different rates of N_2/CO ligand exchange underscore the greater kinetic stability of **2** toward Cr−L dissociative processes that could ultimately curtail catalyst deactivation pathways (i.e. ligand loss) improving catalyst performance for N_2 reduction compared to **1**.

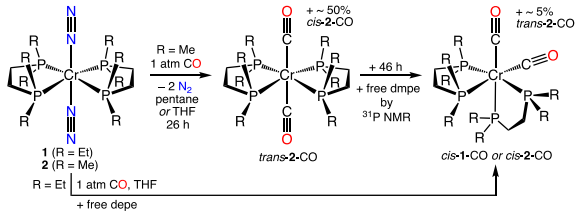

Fig. 3 Ligand exchange reactions of **1** and **2** with CO display different reaction profiles.

In conclusion, we present a contemporary advancement in the use of *trans*-[$Cr(N_2)_2$(P−P)$_2$] complexes (**1** and **2**) for direct catalytic reduction of N_2 to form NH_3 and N_2H_4 using the PCET reagent SmI_2 and H_2O and/or ethylene glycol as proton donors. A new complex, *trans*-[$Cr(N_2)_2$(depe)$_2$], was

presented herein. Despite having similar electronic structures, we posit **2** is a better catalyst than **1** (using the presented conditions), due to a less negative $Cr^{I/0}$ redox couple and greater kinetic stability from Cr–L dissociative processes.

The authors thank Dr. Bernhard Linden and Mathias Linden for LIFDI-MS analysis. This material is based upon work supported by the National Science Foundation (NSF) under Grant No. 1956161. Support for MSU's NMR Center has been provided by the NSF (Grant No. NSF-MRI: CHE-2018388) and MSU's office of the Vice President for Research and Economic Development. The authors gratefully acknowledge financial support for the X-ray diffractometer from the NSF (CHE 0619920) and a Institutional Development Award (IDeA) from the National Institute of General Medical Sciences of the National Institutes of Health (Grant # 2P20GM103432).

Author Contributions

C. Beasley, investigation, methodology, writing, editing; O.L. Duletski, investigation; K.S. Stankevich, investigation; N. Arulsamy, investigation, writing; M.T. Mock, conceptualization, methodology, supervision, writing, editing, funding acquisition.

Conflicts of interest

There are no conflicts of interest to declare.

Notes and references

1. (a) Y. Tanabe and Y. Nishibayashi, *Chem. Soc. Rev.*, 2021, **50**, 5201-5242; (b) Y. Tanabe and Y. Nishibayashi, *Coord. Chem. Rev.*, 2022, **472**, 214783; (c) Y. Nishibayashi, ed., *Transition Metal–Dinitrogen Complexes: Preparation and Reactivity*, Wiley-VCH, Weinheim, 2019.
2. M. J. Chalkley, M. W. Drover and J. C. Peters, *Chem. Rev.*, 2020, **120**, 5582-5636.
3. (a) Y. Ashida, K. Arashiba, K. Nakajima and Y. Nishibayashi, *Nature*, 2019, **568**, 536-540; (b) N. G. Boekell and R. A. Flowers II, *Chem. Rev.*, 2022, **122**, 13447-13477; (c) E. A. Boyd and J. C. Peters, *J. Am. Chem. Soc.*, 2022, **144**, 21337-21346.
4. Y. Ashida, T. Mizushima, K. Arashiba, A. Egi, H. Tanaka, K. Yoshizawa and Y. Nishibayashi, *Nat. Synth.*, 2023, **2**, 635-644.
5. C. Van Stappen, L. Decamps, G. E. Cutsail, III, R. Bjornsson, J. T. Henthorn, J. A. Birrell and S. DeBeer, *Chem. Rev.*, 2020, **120**, 5005-5081.
6. C. M. Goodwin, P. Lomker, D. Degerman, B. Davies, M. Shipilin, F. Garcia-Martinez, S. Koroidov, J. Katja Mathiesen, R. Rameshan, G. L. S. Rodrigues, C. Schlueter, P. Amann and A. Nilsson, *Nature*, 2024, **625**, 282-286.
7. J. Chatt, A. J. Pearman and R. L. Richards, *Nature*, 1975, **253**, 39-40.
8. (a) F. A. Darani, G. P. A. Yap and K. H. Theopold, *Organometallics*, 2023, **42**, 1324-1330; (b) S. J. K. Forrest, B. Schluschass, E. Y. Yuzik-Klimova and S. Schneider, *Chem. Rev.*, 2021, **121**, 6522-6587; (c) C. E. Laplaza and C. C. Cummins, *Science*, 1995, **268**, 861-863.
9. A. Katayama, T. Ohta, Y. Wasada-Tsutsui, T. Inomata, T. Ozawa, T. Ogura and H. Masuda, *Angew. Chem. Int. Ed.*, 2019, **58**, 11279-11284.
10. (a) S. Kim, Y. Park, J. Kim, T. P. Pabst and P. J. Chirik, *Nat. Synth.*, 2022, **1**, 297-303; (b) M. T. Mock, *Nat. Synth.*, 2022, **1**, 262-263.
11. P. Garrido-Barros, J. Derosa, M. J. Chalkley and J. C. Peters, *Nature*, 2022, **609**, 71-76.
12. Y. Ashida, K. Arashiba, H. Tanaka, A. Egi, K. Nakajima, K. Yoshizawa and Y. Nishibayashi, *Inorg. Chem.*, 2019, **58**, 8927-8932.
13. (a) A. J. Kendall and M. T. Mock, *Eur. J. Inorg. Chem.*, 2020, DOI: 10.1002/ejic.201901257, 1358-1375; (b) M. T. Mock, S. Chen, R. Rousseau, M. J. O'Hagan, W. G. Dougherty, W. S. Kassel, D. L. DuBois and R. M. Bullock, *Chem. Commun.*, 2011, **47**, 12212-12214; (c) M. T. Mock, S. Chen, M. O'Hagan, R. Rousseau, W. G. Dougherty, W. S. Kassel and R. M. Bullock, *J. Am. Chem. Soc.*, 2013, **135**, 11493-11496; (d) M. Fritz, S. Demeshko, C. Würtele, M. Finger and S. Schneider, *Eur. J. Inorg. Chem.*, 2023, **26**; (e) W. H. Monillas, G. P. A. Yap, L. A. MacAdams and K. H. Theopold, *J. Am. Chem. Soc.*, 2007, **129**, 8090-8091; (f) W. H. Monillas, G. P. A. Yap and K. H. Theopold, *Inorg. Chim. Acta* 2011, **369**, 103-119; (g) X. Wang, Y. Wang, Y. Wu, G. X. Wang, J. Wei and Z. Xi, *Inorg. Chem.*, 2023, **62**, 18641-18648; (h) M. T. Mock, A. W. Pierpont, J. D. Egbert, M. O'Hagan, S. Chen, R. M. Bullock, W. G. Dougherty, W. S. Kassel and R. Rousseau, *Inorg. Chem.*, 2015, **54**, 4827-4839; (i) J. D. Egbert, M. O'Hagan, E. S. Wiedner, R. M. Bullock, N. A. Piro, W. S. Kassel and M. T. Mock, *Chem. Commun.*, 2016, **52**, 9343-9346; (j) I. Vidyaratne, J. Scott, S. Gambarotta and P. H. M. Budzelaar, *Inorg. Chem.*, 2007, **46**, 7040-7049.
14. (a) J. Yin, J. Li, G. X. Wang, Z. B. Yin, W. X. Zhang and Z. Xi, *J. Am. Chem. Soc.*, 2019, **141**, 4241-4247; (b) G. X. Wang, X. Wang, Y. Jiang, W. Chen, C. Shan, P. Zhang, J. Wei, S. Ye and Z. Xi, *J. Am. Chem. Soc.*, 2023, **145**, 9746-9754; (c) G. X. Wang, Z. B. Yin, J. Wei and Z. Xi, *Acc. Chem. Res.*, 2023, **56**, 3211-3222; (d) Z. B. Yin, B. Wu, G. X. Wang, J. Wei and Z. Xi, *J. Am. Chem. Soc.*, 2023, **145**, 7065-7070; (e) T. Shima, J. Yang, G. Luo, Y. Luo and Z. Hou, *J. Am. Chem. Soc.*, 2020, **142**, 9007-9016; (f) Y. Kokubo, K. Tsuzuki, H. Sugiura, S. Yomura, Y. Wasada-Tsutsui, T. Ozawa, S. Yanagisawa, M. Kubo, T. Takeyama, T. Yamaguchi, Y. Shimazaki, S. Kugimiya, H. Masuda and Y. Kajita, *Inorg. Chem.*, 2023, **62**, 5320-5333.
15. (a) A. J. Kendall, S. I. Johnson, R. M. Bullock and M. T. Mock, *J. Am. Chem. Soc.*, 2018, **140**, 2528-2536; (b) M. C. Eaton, B. J. Knight, V. J. Catalano and L. J. Murray, *Eur. J. Inorg. Chem.*, 2020, 1519-1524; (c) J. Li, J. Yin, G. X. Wang, Z. B. Yin, W. X. Zhang and Z. Xi, *Chem. Commun.*, 2019, **55**, 9641-9644.
16. Y. Ashida, A. Egi, K. Arashiba, H. Tanaka, T. Mitsumoto, S. Kuriyama, K. Yoshizawa and Y. Nishibayashi, *Chem. Eur. J.*, 2022, **28**, e202200557.
17. (a) G. S. Girolami, J. E. Salt, G. Wilkinson, M. Thornton-Pett and M. B. Hursthouse, *J. Am. Chem. Soc.*, 1983, **105**, 5954-5956; (b) J. E. Salt, G. S. Girolami, G. Wilkinson, M. Motevalli, M. Thornton-Pett and M. B. Hursthouse, *J. Chem. Soc. Dalton Trans.*, 1985, 685-692.
18. D. M. Halepoto, D. G. L. Holt, L. F. Larkworthy, G. J. Leigh, D. C. Povey and G. W. Smith, *J. Chem. Soc. Chem. Commun.*, 1989, 1322-1323.
19. Structural metrics from XRD data of **2** collected here at 100 K. Data from ref 17 at 295 K.
20. (a) M. L. Kuhlman and R. A. Flowers II, *Tetrahedron Lett.*, 2000, **41**, 8049-8052; (b) R. J. Enemærke, K. Daasbjerg and T. Skrydstrup, *Chem. Commun.*, 1999, 343-344.
21. J. E. Salt, G. Wilkinson, M. Motevalli and M. B. Hursthouse, *J. Chem. Soc. Dalton Trans.*, 1986, 1141-1154.
22. (a) J. Rittle and J. C. Peters, *J. Am. Chem. Soc.*, 2016, **138**, 4243-4248; (b) N. B. Thompson, P. H. Oyala, H. T. Dong, M. J. Chalkley, J. Zhao, E. E. Alp, M. Hu, N. Lehnert and J. C. Peters, *Inorg. Chem.*, 2019, **58**, 3535-3549.